

RESEARCH ARTICLE

Diagnostic efficacy of CBCT, MRI and CBCT–MRI fused images in determining anterior disc displacement and bone changes of temporomandibular joint

^{1,2}Ying-Hui Wang, ^{1,2}Ruo-Han Ma, ³Jia-Jun Li, ^{1,2}Chuang-Chuang Mu, ^{1,2,4}Yan-Ping Zhao, ^{2,4}Juan-Hong Meng and ^{1,2}Gang Li

¹Department of Oral and Maxillofacial Radiology, Peking University School and Hospital of Stomatology, Beijing, China; ²National Center of Stomatology & National Clinical Research Center for Oral Diseases & National Engineering Laboratory for Digital and Material Technology of Stomatology & Beijing Key Laboratory of Digital Stomatology & Research Center of Engineering and Technology for Computerized Dentistry Ministry of Health & NMPA Key Laboratory for Dental Materials, Beijing, China; ³The affiliated high school of Peking University, Beijing, China; ⁴Center for Temporomandibular Disorders and Orofacial Pain, Peking University School and Hospital of Stomatology, Beijing, China

Objectives: To evaluate the diagnostic efficacy of CBCT–MRI fused image for anterior disc displacement and bone changes of temporomandibular joint (TMJ), which are the main imaging manifestations of temporomandibular disorders (TMD).

Methods: Two hundred and thirty-one TMJs of 120 patients who were diagnosed with TMD were selected for the study. The anterior disc displacement, bone defect and bone hyperplasia evaluated by three experts were used as a reference standard. Three residents individually evaluated all the three sets of images, which were CBCT images, MRI images and CBCT-MRI fused images from individual CBCT and MRI images in a random order for the above-mentioned three imaging manifestations with a five-point scale. Each set of images was observed at least 1 week apart. A second evaluation was performed 4 weeks later. Intra- and inter observer agreements were assessed using the intraclass correlation coefficient (ICC). The areas under the ROC curves (AUCs) of the three image sets were compared with a Z test, and $p < 0.05$ was considered statistically significant.

Results: One hundred and forty-five cases were determined as anterior disc displacement, 84 cases as bone defect and 40 cases as bone hyperplasia. The intra- and inter observer agreements in the CBCT-MRI fused image set (0.76–0.91) were good to excellent, and the diagnostic accuracy for bone changes was significantly higher than that of MRI image set ($p < 0.05$).

Conclusions CBCT-MRI fused images can display the disc and surrounding bone structures simultaneously and significantly improve the observers' reliability and diagnostic accuracy, especially for inexperienced residents.

Dentomaxillofacial Radiology (2022) **51**, 20210286. doi: [10.1259/dmfr.20210286](https://doi.org/10.1259/dmfr.20210286)

Cite this article as: Wang Y-H, Ma R-H, Li J-J, Mu C-C, Zhao Y-P, Meng J-H, et al. Diagnostic efficacy of CBCT, MRI and CBCT–MRI fused images in determining anterior disc displacement and bone changes of temporomandibular joint. *Dentomaxillofac Radiol* 2022; **51**: 20210286.

Keywords: temporomandibular joint; diagnosis; Cone-Beam Computed Tomography; magnetic resonance imaging

Introduction

Temporomandibular disorders (TMD) affect approximately 5 to 12% of the population. It can cause chronic pain and dysfunction in the joint and its associated muscles and supporting tissues.¹ Correct diagnosis is very important for the treatment of TMD to avoid pain and disability. The diagnostic criteria for the most common TMD (DC/TMD) are based on symptom questionnaire and clinical examination. Without imaging examination, the diagnostic sensitivity of the common TMD is low, except for “Disc displacement without reduction with limited opening”.² The American Association for Dental Research states that various imaging modalities show the sensitivity and specificity required to separate normal subjects from TMD patients or to distinguish among TMD subgroups.³

Temporomandibular joint (TMJ) imaging examination is mainly used for diagnosis of various joint disc displacement and degenerative joint diseases (osteoarthropathy).⁴ Cone-beam computed tomography (CBCT) is increasingly being used as an imaging modality in the assessment of the TMJ due to its high spatial resolution,⁵ high diagnostic accuracy of surface osseous changes in condyle and temporal bone,⁶ low radiation dose and low cost.^{6–8} CBCT can comprehensively reflect the bone changes of TMJ (erosion, flattening, osteophytes, hypoplasia, sclerosis and subchondral cyst).⁹ Whereas it has low density resolution and poor imaging ability for soft tissue and its space. Therefore, other imaging examinations, such as magnetic resonance imaging (MRI), are needed when the soft tissue lesions of TMJ are suspected. MRI is used to evaluate the position and shape of the disc, the presence/absence of fluid within the joint space (joint effusion), the marrow signal of the condyle and pannus formation (in the case of inflammatory arthritides).^{10,11}

However, both CBCT and MRI have shortcomings in enabling the clinician to effectively visualize the TMJ structures. Therefore, a method used to fuse CBCT and MRI images was established. In order to make a comprehensive and accurate diagnosis of TMD, researchers have made a variety of explorations, trying to register CBCT and MRI images so that both soft and hard tissues can be displayed simultaneously.^{12–16} Lin *et al*¹⁴ placed markers in bilateral TMJ area and chin for CT and MRI scanning and three-dimensional reconstruction. Dai *et al*¹⁵ integrated CBCT with MRI image using anatomical markers of the TMJ in the Photoshop CS4 software. He *et al*¹⁶ used condyles as internal markers for

CBCT-MRI image registration. Al-Saleh *et al*¹⁷ reconstructed the three-dimensional surface model of soft and hard tissues of TMJ after fusing MRI and CBCT images to evaluate the changes of disc and condyle position and condyle-disc relationship after mandibulotomy. Al-Saleh *et al*¹⁸ and Ma *et al*¹⁹ fused CBCT and MRI images based on mutual information to diagnose TMD and other related joint diseases.

With the merits of applying fused images for the diagnosis of TMD, limitations are also presented in the previous studies. For example, the sample size was small, only a few to dozens of cases were involved; different fusion methods were used in different studies, and the diagnostic value of fused images varied greatly. Thus, the purposes of the present study were to establish a 3D multimodal medical image registration and fusion method for TMJ, and to evaluate the diagnostic efficacy of CBCT-MRI fused images for anterior disc displacement and bone changes, which are the main imaging manifestations of TMD.

Methods and materials

Subjects

Previous study has shown that the clinical detection rate of TMD in Chinese was about 54.2%.²⁰ Assuming that both sensitivity and specificity for the imaging detection of TMD were 0.9, 100 positive cases were needed at least.

CBCT and MRI images taken from the patients who firstly visited the Center for Temporomandibular Disorders and Orofacial Pain in Peking University School and Hospital of Stomatology from 2016 to 2020 were reviewed. The inclusion criteria were: (1) the patient was diagnosed as TMD with medical history, physical and imaging examinations; (2) for diagnostic purpose, the patient had taken CBCT and MRI images at a time interval within one month; (3) no other temporomandibular joint diseases such as tumor, trauma, joint ankylosis, joint dislocation or infectious arthritis in oral and maxillofacial region.

The exclusion criteria were: (1) the patient was not diagnosed as TMD according to the clinical diagnostic criteria; (2) patient only had single CBCT or MRI images, or both were not taken at the same period of time; (3) there are other temporomandibular joint diseases such as tumor, trauma, joint ankylosis, joint

Table 1 Scanning parameters used in CBCT images of TMJ

Unit	Tube Voltage (kVp)	Tube Current (mA)	Scan Time (s)	FOV (mm ²)	Voxel Size (mm)
3D Accuitomo 170	80–90	4–5	17.5	60 × 60	0.125
NewTom VGi	110	1–5	18.0	150 × 150/150 × 120	0.250
i-CAT FLX	120	5	8.9	160 × 130	0.300

CBCT, Cone-beam computed tomography; FOV, Field of view; TMJ, Temporomandibular joint.

Table 2 Scanning parameters used in MRI images of TMJ

Sequence	Orientation	TR (ms)	TE (ms)	FOV (mm ²)	Slice Thickness (mm)	Interslice Gap Spacing (mm)	Pixel Size (mm)
T2WI	Axial	3700	90	220 × 220	3	0.6	0.430
PD/T2WI	Oblique sagittal	4120	20/99	140 × 140	3	0.3	0.547
T1WI	Oblique sagittal	250	2.7	140 × 140	3	0.3	0.438
T2WI	Oblique coronal	2000	86	140 × 140	3	0.3	0.438

FOV, Field of view; MRI, Magnetic resonance imaging; PDWI, Proton density weighted imaging; TE, Echo time; TMJ, Temporomandibular joint; TR, Repetition time; T₁WI, T₁ weighted imaging; T₂WI, T₂ weighted imaging.

dislocation or infectious arthritis in oral and maxillo-facial region.

CBCT and MRI image acquisition

The CBCT unit rotated 360° with the patients sitting or standing in the upright position with the Frankfort plane parallel to the floor. The thyroid collar was used. Images of each TMJ were obtained in the maximal intercuspation. Scans were performed using 3D Accuitomo 170 (J. Morita MFG. Corp., Kyoto, Japan), NewTom VGi (Quantitative Radiology, Verona, Italy) or i-CAT FLX (Imaging Sciences International Inc., Hatfield, PA, USA). The scanning parameters of each CBCT unit are shown in Table 1.

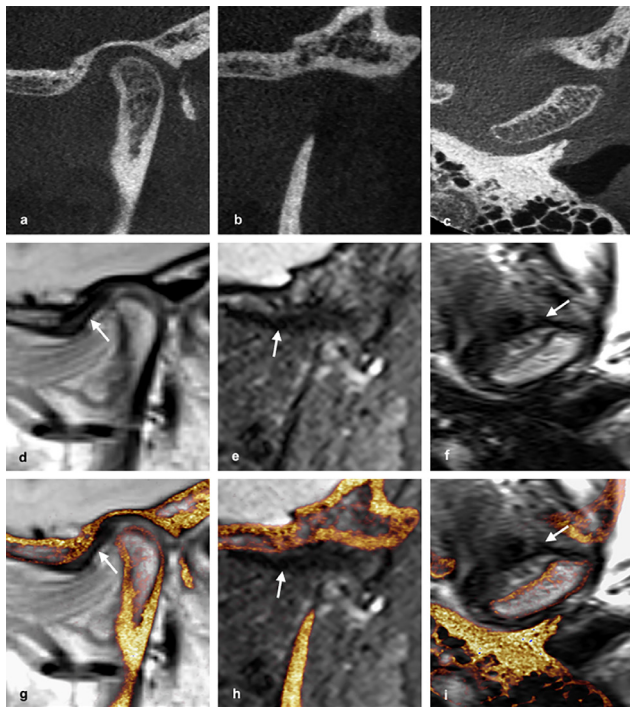


Figure 1 Example images for the anterior disc displacement of TMJ (arrows). Oblique sagittal (a), oblique coronal (b) and axial (c) view of the CBCT images; Oblique sagittal view of the MRI image in PDWI (d), oblique coronal (e) and axial (f) view of the MRI images in T₂WI; Oblique sagittal view of the CBCT-MRI (PDWI) fused image (g); Oblique coronal (h) and axial (i) view of the CBCT-MRI (T₂WI) fused images. TMJ: temporomandibular joint; CBCT, cone-beam CT; MRI, magnetic resonance imaging; PDWI, proton density weighted imaging; T₂WI, T₂-weighted imaging.

Each MRI scan was acquired in the supine position using Siemens 3T TIM Trio magnet (Siemens Medical Solutions, Erlangen, Germany) with coils on 32 independent receiver channels. No sedation or intravenous contrast administration was used. Patients were scanned in axial, oblique sagittal position which is perpendicular to the long axis of the condyle, and oblique coronal position which is parallel to the long axis of the condyle. Images were obtained in both maximal intercuspation and maximal voluntary interincisal mouth opening position. Scanning parameters of different sequences are shown in Table 2.

All the image data sets obtained from CBCT and MRI unit were exported as digital imaging and communications in medicine (DICOM) format.

Imaging registration and fusion

Image registration and fusion of CBCT and MRI images was carried out using the Amira software (version 2020.2, Thermo Scientific, France), and the registration process was conducted in the multiplanar viewer module. First, MRI images were resampled to the same voxel size as to the corresponding CBCT images. Then, the operator adjusted two image sets to align position roughly by using the manual registration tool. The imaging principles differs among CBCT and MRI images, resulting in differences in voxel size, pixel intensity, anatomical structure identification, image orientation and field of view (FOV). Thus, similarity metric of normalized mutual information (NMI) and rigid transform model were used. The conjugated gradient method was chosen as the optimizer. In the end, design the parameter to make the registration process faster and more precise. The detailed information was described in our previous study.¹⁹ In CBCT-MRI fused images, the floating images (CBCT) were colored in luminous yellow and the reference images (MRI) in gray-scale.

Image evaluation

The expert panel consisted of one specialist with an experience of over 25 years in oral and maxillofacial radiology and two certified specialists with an experience of over 30 years in temporomandibular disorders and orofacial pain. The specialists individually determined whether the patient had anterior disc displacement, bone defect or bone hyperplasia based on patient information, which included the medical history,

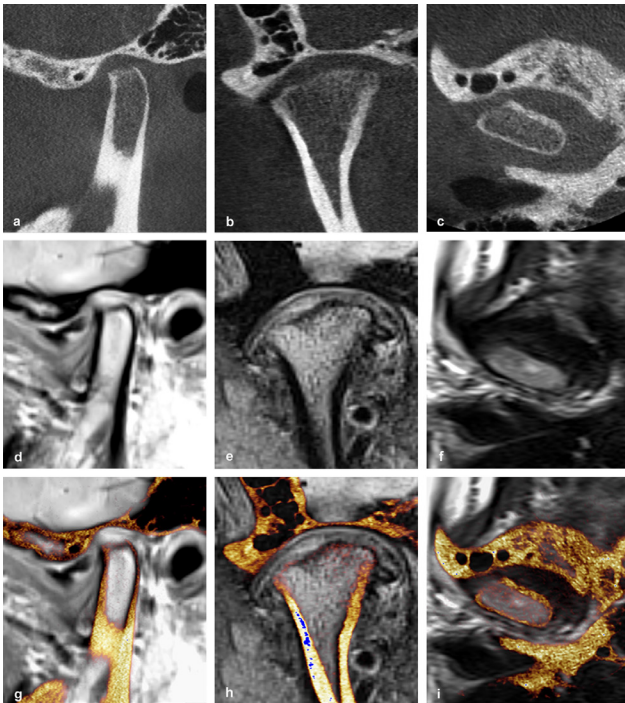


Figure 2 Example images for the bone defect of TMJ. Oblique sagittal (a), oblique coronal (b) and axial (c) view of the CBCT images; Oblique sagittal view of the MRI image in PDWI (d), oblique coronal (e) and axial (f) view of the MRI images in T_2 WI; Oblique sagittal view of the CBCT-MRI (PDWI) fused image (g); Oblique coronal (h) and axial (i) view of the CBCT-MRI (T_2 WI) fused images. TMJ: temporomandibular joint; CBCT, cone-beam CT; MRI, magnetic resonance imaging; PDWI, proton density-weighted imaging; T_2 WI, T_2 weighted imaging.

physical examination, and image examinations (CBCT images, MRI images and CBCT-MRI fused images). In the end, in all cases, consensus was reached among the three specialists. The diagnosis of anterior disc displacement, bone defect and bone hyperplasia evaluated by the expert panel was used as a reference standard.

Three oral and maxillofacial radiology residents acted as observers, all of whom had at least 3 years of experience. The theory of the image fusion technique, the MRI images and CBCT-MRI fused images of TMJ were explained to observers before each evaluation as a calibration session.

Three residents evaluated the bone defect and bone hyperplasia of TMJs in three sets of images (CBCT images alone, MRI images alone and CBCT-MRI fused images), and anterior disc displacement in two image sets (MRI images alone and CBCT-MRI fused images) randomly and independently. To reduce recall bias, different image sets from a same patient were examined at least one week apart. The observers assessed the images on a five-point scale: 1- definitely not anterior disc displacement, bone defect or bone hyperplasia; 2- probably not anterior disc displacement, bone defect or bone hyperplasia; 3- questionable; 4- probably anterior disc displacement, bone defect or bone hyperplasia;

5- definitely anterior disc displacement, bone defect or bone hyperplasia.

All images were viewed on Nio Color 5.8 MP (MDNC-6121) display (Barco, Kortrijk, Belgium) under dim lighting conditions. The image datasets of 231 TMJs were numbered as #1C-#231C (CBCT images), #1M-#231M (MRI images) and #1F-#231F (CBCT-MRI fused images). To avoid viewing fatigue, the images were randomly divided into 10 groups and only one group of images was assessed at each time. Images can be modified by adjusting the orientation, color gradient, brightness, contrast and magnification to reach the best display. There is no time limit on the evaluation process. To evaluate the intra observer agreement, 20% of each image sets were randomly selected to reassess 4 weeks later.

Statistical analysis

Sample size calculation was made with Power Analysis and Sample Size (PASS) software package V.11.0 (NCSS, LLC, Kaysville, Utah, USA). Data analysis was performed with IBM SPSS Statistics for Windows V.20.0 (IBM Corp., Armonk, New York, USA). A *p* value of 0.05 or less was considered statistically significant. Intra- and inter observer agreements were assessed

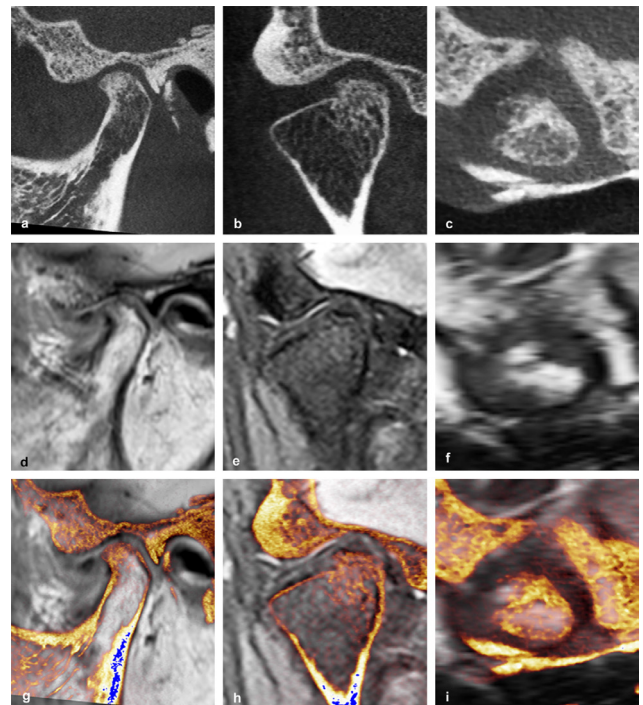


Figure 3 Example images for the bone hyperplasia of TMJ. Oblique sagittal (a), oblique coronal (b) and axial (c) view of the CBCT images; Oblique sagittal view of the MRI image in PDWI (d), oblique coronal (e) and axial (f) view of the MRI images in T_2 WI; Oblique sagittal view of the CBCT-MRI (PDWI) fused image (g); Oblique coronal (h) and axial (i) view of the CBCT-MRI (T_2 WI) fused images. TMJ: temporomandibular joint; CBCT, cone-beam CT; MRI, magnetic resonance imaging; PDWI, proton density-weighted imaging; T_2 WI, T_2 -weighted imaging.

Table 3 Intra-observer agreement for each of the three image sets (ICC)

Observer	Anterior disc displacement			Bone defect			Bone hyperplasia		
	MRI	CBCT-MRI	CBCT	MRI	CBCT-MRI	CBCT	MRI	CBCT-MRI	
1	0.57	0.85	0.91	0.69	0.83	0.81	0.32	0.78	
2	0.58	0.90	0.82	0.47	0.85	0.71	0.44	0.76	
3	0.65	0.83	0.87	0.55	0.87	0.87	0.43	0.75	
Mean	0.60	0.86	0.87	0.57	0.85	0.80	0.40	0.76	

CBCT, Cone-beam computed tomography; CBCT-MRI, CBCT-MRI fused image set; ICC, Intraclass correlation coefficients; MRI, Magnetic resonance imaging.

ICC values²¹: agreement was rated as “poor” (<0.50), “moderate” (0.50–0.75), “good” (0.75–0.90), and “excellent” (>0.90).

using the intraclass correlation coefficient (ICC). The criteria for ICC values classification were: <0.50 as poor, 0.50–0.75 as moderate, 0.75–0.90 as good and >0.90 was considered as excellent.²¹ Receiver operating characteristic (ROC) curves for each image set were generated by pooling the results of three observers. The areas under the curves (AUCs) comparison were performed by MedCalc15.2.2 (MedCalc Software, Ostend, Belgium) with Z test.

Results

In total, 120 patients (231 TMJs) with a mean age of 31.5 ± 16.28 (age range: 13–85) years old were included, of which 28 (23.3%) patients were male, 92 (76.7%) female. Duration of disease ranged from 2 months to 5 years. All these patients received conservative treatment rather than surgery.

Nine TMJs in 120 patients (240 TMJs) were excluded because of unclear display of articular disc degeneration or failure of CBCT and MRI registration. One hundred and forty-five cases were determined as anterior disc displacement (Figure 1), among which 43 cases were with reduction, 102 cases were without reduction. Eighty-four cases were determined as bone defect (Figure 2), 40 cases as bone hyperplasia (Figure 3) by the expert panel.

The intra- and inter observer agreements of the residents with regard to different image sets are presented in Tables 3 and 4. For intra observer agreement of the detection of anterior disc displacement, ICC values were good for the CBCT-MRI fused image set (0.86), while moderate for MRI image set (0.60). For intra observer agreement of the detection of bone changes, ICC values were good for both CBCT (0.87 for bone defect, 0.80

for bone hyperplasia) and CBCT-MRI fused image sets (0.85 for bone defect, 0.76 for bone hyperplasia), while poor to moderate for MRI images (0.57 for bone defect, 0.40 for bone hyperplasia). The inter observer agreements in the CBCT-MRI fused image set (0.85–0.91) were good to excellent in evaluation of anterior disc displacement and bone changes, higher than those in the other image sets.

ROC curves drawn on the basis of pooled data from the three observers for each of these image sets are shown in Figures 4–6. Table 5 presents the AUC values according to image sets and imaging manifestations. The AUCs for the CBCT-MRI fused image set (0.87 for bone defect, 0.85 for bone hyperplasia) and CBCT image set (0.86 for bone defect, 0.81 for bone hyperplasia) were significantly higher than the MRI image set (0.76 for bone defect, 0.75 for bone hyperplasia) in detection of bone changes ($p < 0.05$). For the diagnosis of anterior disc displacement, the AUC value for the CBCT-MRI fused image set (0.92) was higher than that of MRI image set (0.90), but not significantly different ($p > 0.05$). p values when comparing AUC of each image set are shown in Table 6.

Discussion

Mutual information method was first introduced into the field of medical image registration by Maes et al²². It measures the statistical dependence or information redundancy between the image intensities of corresponding voxels in both images. When the images are geometrically aligned, mutual information is maximal.²² Maximization of mutual information can improve the accuracy and robustness of multi mode image registration without any prior segmentation, feature extraction,

Table 4 Inter observer agreement for each of the three image sets [ICC (95% CI)]

	Anterior disc displacement	Bone defect	Bone hyperplasia
CBCT	–	0.84 (0.79, 0.92)	0.71 (0.62, 0.77)
MRI	0.87 (0.83, 0.90)	0.70 (0.62, 0.77)	0.69 (0.61, 0.75)
CBCT-MRI	0.91 (0.88, 0.93)	0.85 (0.81, 0.89)	0.85 (0.81, 0.88)

CBCT, Cone-beam computed tomography; CBCT-MRI, CBCT-MRI fused image set; ICC, Intraclass correlation coefficient; MRI, Magnetic resonance imaging.

ICC values²¹: agreement was rated as “poor” (<0.50), “moderate” (0.50–0.75), “good” (0.75–0.90), and “excellent” (>0.90).

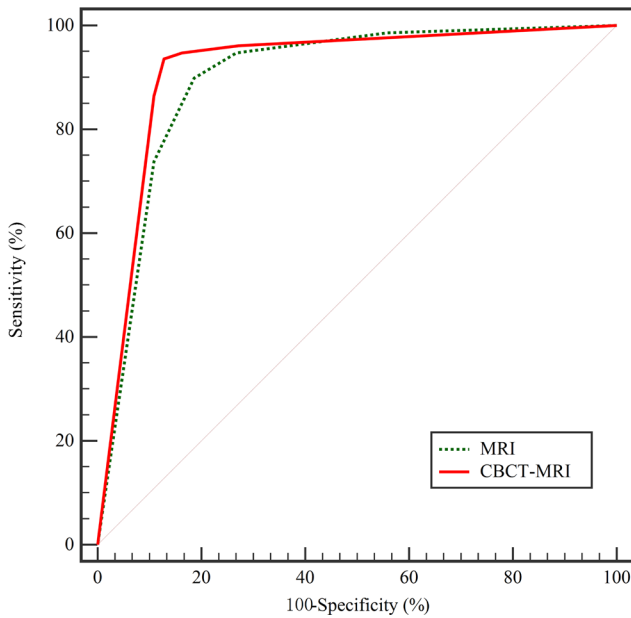


Figure 4 Receiver operating characteristic curves for the two image sets from pooled data for anterior disc displacement of TMJ. TMJ, Temporomandibular joint.

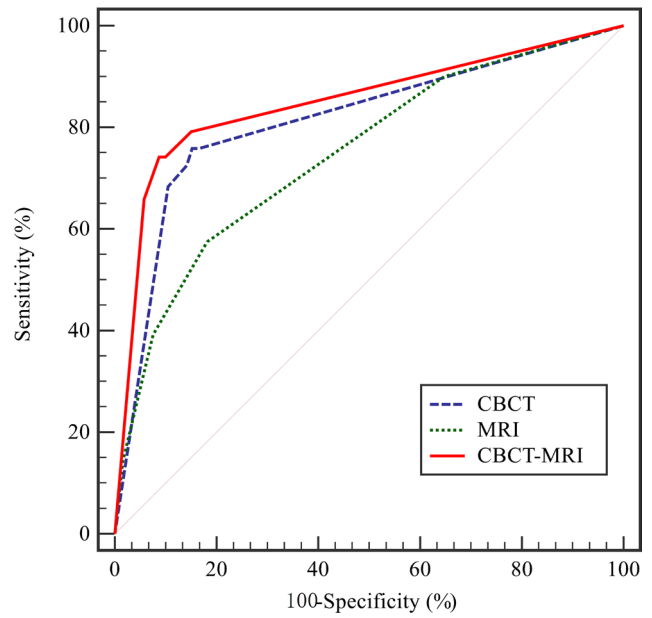


Figure 6 Receiver operating characteristic curves for the three image sets from pooled data for bone hyperplasia of TMJ. TMJ, Temporomandibular joint.

or other preprocessing steps.^{22,23} Studholme *et al*²⁴ developed normalized mutual information (NMI) to decrease sensitivity to image overlap, where large misalignments can occur with respect to the FOV between images from different modalities. The effectiveness of NMI has been confirmed in the previous studies,^{19,25} and also identified in the present study.

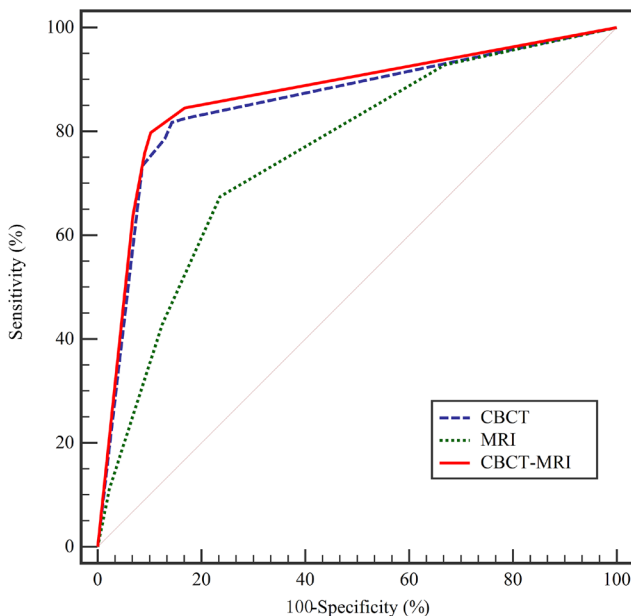


Figure 5 Receiver operating characteristic curves for the three image sets from pooled data for bone defect of TMJ. TMJ, Temporomandibular joint.

In the present study, the estimated diagnostic accuracy of anterior disc displacement was higher for the CBCT-MRI fused images than for the MRI images, but no statistical difference was found. This is contrast to the previous study in which 16 TMJs were evaluated with regard to the anterior disc displacement by 30 students and two expert radiologists. The agreement between the students' value and the true values determined by the expert radiologists was improved from poor agreement with MRI images alone to moderate agreement with CBCT-MRI fused images ($p < 0.001$).¹⁸ The reason may be due to the fact that a considerably large number of subjects (231 TMJs) was employed in the present study and a ROC analysis was used for the data analysis while in the previous study the “not clear” scores were not included in the final statistical analysis.

The intra- and inter observer agreements for anterior disc displacement is moderate to good for MRI images, while good to excellent for CBCT-MRI fused images. The improvement is in consistent with the previous researches by Al-Saleh *et al*^{12,18,26}. The inter observer agreements for both the MRI and CBCT-MRI fused images were relatively higher than the intra observer agreements in this study. This is because of the ICC models used for the calculation. The intra observer agreement was calculated based on a single-rating model, while the inter observer agreement was based on a mean-rating model. In this sense, the inter and intra observer agreement should not be put together for comparison.

As for the bone changes, the diagnostic accuracy of MRI images is significantly lower than those of the CBCT images, which is also identified by other study,²⁷

Table 5 Area under the ROC curve (AUC [95% CI]) for the three image sets

	<i>Anterior disc displacement</i>	<i>Bone defect</i>	<i>Bone hyperplasia</i>
CBCT	–	0.86 (0.83, 0.88)	0.81 (0.78, 0.84)
MRI	0.90 (0.87, 0.92)	0.76 (0.72, 0.79)	0.75 (0.71, 0.78)
CBCT-MRI	0.92 (0.89, 0.94)	0.87 (0.84, 0.89)	0.85 (0.82, 0.88)

CBCT, Cone-beam computed tomography; CBCT-MRI, CBCT-MRI fused image set; MRI, Magnetic resonance imaging; ROC, Receiver operating characteristic.

as well as the fused images in the present study. The intra- and inter observer agreements were relatively high (moderate to good) among the observers for the CBCT and CBCT-MRI fused images in diagnosis of bone changes. This is in line with the study by Al-Saleh *et al*¹², in which the frequency of reporting bone abnormalities in CBCT and CBCT-MRI fused images are similar between three radiologists. It is worth mentioning that fused images not only presented a similar diagnostic accuracy and inter observer consistency to CBCT images,¹² but also showed slightly higher diagnostic accuracy of bone hyperplasia. The possible explanation may be in that CBCT as a floating image in the fused image can reduce noise interference from the soft tissues by adjusting the contrast so that the bone cortex of condyle is displayed clearly and intuitively. This may help in assessing bony abnormality.

In the present study, the number of patients involved was calculated based on the clinical detection rate of TMD. This makes the results from the present study confidential. Due to the conservative treatment of temporomandibular disorders, no pathological or arthroscopic examination was done for the patients and thus no pathological or arthroscopic results can be used as the gold standard for the evaluation of diagnostic accuracy. However, this is a very common problem for clinical studies that do not require surgical treatment. Also, researchers have found that the diagnostic results of MRI images are reliable only if they are calibrated by experienced observers and derived as a group.²⁸ Therefore, in the present study, the results from the three specialists' assessment in anterior disc displacement and bone changes were used as a reference standard.

One limitation of the study is the observers employed for the image evaluation. They are all residents with three years of experience. The accuracy and reliability of diagnosis may be different

among the observers with different qualifications. However, when we consider other similar studies in which student observers,¹⁸ radiologists with five-year working experience,¹² and radiologists with 7–8 year working experience²⁶ were employed for the evaluation of CBCT-MRI fused images and similar results are performed, the diagnostic reliability of CBCT-MRI fused images may be confirmed.

Another limitation is that the traditional iterative registration method based on mutual information has excellent robustness and accuracy, but large calculation amount and long time consuming makes it difficult to ensure a real-time application in practical. In addition, fusing CBCT and MRI images need to manually preregister the two images in the early stage of operation to avoid local optima which may lead to registration failure.²⁹ Therefore, the quality of the fused image not only depends on the operator's experience, but also the registration process. The future research may be to find an automatic registration method, such as deep learning method, to overcome the current shortcomings.

Conclusions

CBCT-MRI fused images can significantly improve the observers' reliability in determining anterior disc displacement and bone changes of TMJ. It can also be utilized especially for inexperienced residents to improve diagnostic efficacy.

Competing interests

The authors declare that they have no conflict of interest.

Table 6 *p* values when comparing AUC of each image set

	<i>Anterior disc displacement</i>		<i>Bone defect</i>		<i>Bone hyperplasia</i>	
	<i>MRI</i>	<i>CBCT-MRI</i>	<i>MRI</i>	<i>CBCT-MRI</i>	<i>MRI</i>	<i>CBCT-MRI</i>
CBCT	–	–	0.00 ^a	0.32	0.03 ^a	0.06
MRI	–	0.13	–	0.00 ^a	–	0.00 ^a

AUC, Area under the curve; CBCT, Cone-beam computed tomography; CBCT-MRI, CBCT-MRI fused image set; MRI, Magnetic resonance imaging.

^aSignificant difference between two image sets for AUC.

Funding

The study was supported by National Natural Science Foundation of China (No. 81671034).

Ethics approval

All procedures performed in the study involving human participants were in accordance with the ethical

standards of Institutional Review Board of Peking University School and Hospital of Stomatology and with the 1964 Helsinki declaration and its later amendments or comparable ethical standards. The study was approved by the Institutional Review Board of Peking University School and Hospital of Stomatology (PKUSSIRB-201944056).

REFERENCES

- National Institute of Dental and Craniofacial Research. Facial pain. 2018. Available from: <https://www.nidcr.nih.gov/research/data-statistics/facial-pain>.
- Schiffman E, Ohrbach R, Truelove E, Look J, Anderson G, Goulet J-P, et al. Diagnostic criteria for temporomandibular disorders (DC/TMD) for clinical and research applications: recommendations of the International RDC/TMD Consortium Network* and orofacial pain special interest Group†. *J Oral Facial Pain Headache* 2014; **28**: 6–27. doi: <https://doi.org/10.11607/jop.1151>
- Greene CS. American association for dental research. diagnosis and treatment of temporomandibular disorders: emergence of a new care guidelines statement. *Oral Surg Oral Med Oral Pathol Oral Radiol Endo* 2010; **110**: 137–9.
- Fu KY. Necessity and normalization of imaging examination on temporomandibular disorders. *Zhonghua Kou Qiang Yi Xue Za Zhi* 2019; **54**: 505–9. doi: <https://doi.org/10.3760/cma.j.issn.1002-0098.2019.08.001>
- Krishnamoorthy B, Mamatha N, Kumar VA. TMJ imaging by CBCT: current scenario. *Ann Maxillofac Surg* 2013; **3**: 80–3. doi: <https://doi.org/10.4103/2231-0746.110069>
- Zain-Alabdeen EH, Alsadhan RI. A comparative study of accuracy of detection of surface osseous changes in the temporomandibular joint using multidetector CT and cone beam CT. *Dentomaxillofac Radiol* 2012; **41**: 185–91. doi: <https://doi.org/10.1259/dmfr/24985971>
- Honda K, Larheim TA, Maruhashi K, Matsumoto K, Iwai K. Osseous abnormalities of the mandibular condyle: diagnostic reliability of cone beam computed tomography compared with helical computed tomography based on an autopsy material. *Dentomaxillofac Radiol* 2006; **35**: 152–7. doi: <https://doi.org/10.1259/dmfr/15831361>
- Hashimoto K, Arai Y, Iwai K, Araki M, Kawashima S, Terakado M. A comparison of a new limited cone beam computed tomography machine for dental use with a multidetector row helical CT machine. *Oral Surg Oral Med Oral Pathol Oral Radiol Endod* 2003; **95**: 371–7. doi: <https://doi.org/10.1067/moe.2003.120>
- Cömert Kiliç S, Kiliç N, Sümbüllü MA. Temporomandibular joint osteoarthritis: cone beam computed tomography findings, clinical features, and correlations. *Int J Oral Maxillofac Surg* 2015; **44**: 1268–74. doi: <https://doi.org/10.1016/j.ijom.2015.06.023>
- Talmaceanu D, Lenghel LM, Bolog N, Hedesiu M, Buduru S, Rotar H, et al. Imaging modalities for temporomandibular joint disorders: an update. *Chujl Med* 2018; **91**: 280–7. doi: <https://doi.org/10.15386/cjmed-970>
- Hunter A, Kalathingal S. Diagnostic imaging for temporomandibular disorders and orofacial pain. *Dent Clin North Am* 2013; **57**: 405–18. doi: <https://doi.org/10.1016/j.cden.2013.04.008>
- Al-Saleh MAQ, Jaremko JL, Alsufyani N, Jibri Z, Lai H, Major PW. Assessing the reliability of MRI-CBCT image registration to visualize temporomandibular joints. *Dentomaxillofac Radiol* 2015; **44**: 20140244. doi: <https://doi.org/10.1259/dmfr.20140244>
- Al-Saleh MAQ, Punithakumar K, Jaremko JL, Alsufyani NA, Boulanger P, Major PW. Accuracy of magnetic resonance imaging-cone beam computed tomography rigid registration of the head: an in-vitro study. *Oral Surg Oral Med Oral Pathol Oral Radiol* 2016; **121**: 316–21. doi: <https://doi.org/10.1016/j.oooo.2015.10.029>
- Lin Y-L, Liu Y-H, Wang D-M, Wang C-T. Three-dimensional reconstruction of temporomandibular joint with CT and MRI medical image fusion technology. *Hua Xi Kou Qiang Yi Xue Za Zhi* 2008; **26**: 140–3.
- Dai J, Dong Y, Shen SG. Merging the computed tomography and magnetic resonance imaging images for the visualization of temporomandibular joint disc. *J Craniofac Surg* 2012; **23**: e647–8. doi: <https://doi.org/10.1097/SCS.0b013e3182710517>
- He YM, Wang HY, Feng YP, Li HM, Fang W, Ke J, et al. A preliminary study on the registration of MRI and cone beam CT images of temporomandibular joint disc. *Zhonghua Kou Qiang Yi Xue Za Zhi* 2020; **55**: 772–7. doi: <https://doi.org/10.3760/cma.j.cn112144-20200605-00319>
- Al-Saleh MAQ, Punithakumar K, Lagravere M, Boulanger P, Jaremko JL, Wolfaardt J, et al. Three-Dimensional morphological changes of the temporomandibular joint and functional effects after mandibulotomy. *J Otolaryngol Head Neck Surg* 2017; **46**: 8. doi: <https://doi.org/10.1186/s40463-017-0184-4>
- Al-Saleh MAQ, Alsufyani N, Lai H, Lagravere M, Jaremko JL, Major PW. Usefulness of MRI-CBCT image registration in the evaluation of temporomandibular joint internal derangement by novice examiners. *Oral Surg Oral Med Oral Pathol Oral Radiol* 2017; **123**: 249–56. doi: <https://doi.org/10.1016/j.oooo.2016.10.016>
- Ma R-H, Li G, Sun Y, Meng J-H, Zhao Y-P, Zhang H. Application of fused image in detecting abnormalities of temporomandibular joint. *Dentomaxillofac Radiol* 2019; **48**: 20180129. doi: <https://doi.org/10.1259/dmfr.20180129>
- Wang Y, XC M, Li C, Wang WY. Prevalence of temporomandibular disorders in 1006 General subjects in Beijing (article in Chinese). *Xian Dai Kou Qiang Yi Xue Za Zhi* 2000; **14**: 113–6.
- Koo TK, Li MY. A guideline of selecting and reporting intra-class correlation coefficients for reliability research. *J Chiropr Med* 2016; **15**: 155–63. doi: <https://doi.org/10.1016/j.jcm.2016.02.012>
- Maes F, Collignon A, Vandermeulen D, Marchal G, Suetens P. Multimodality image registration by maximization of mutual information. *IEEE Trans Med Imaging* 1997; **16**: 187–98. doi: <https://doi.org/10.1109/42.563664>
- Maes F, Vandermeulen D, Suetens P. Comparative evaluation of multiresolution optimization strategies for multimodality image registration by maximization of mutual information. *Med Image Anal* 1999; **3**: 373–86. doi: [https://doi.org/10.1016/S1361-8415\(99\)80030-9](https://doi.org/10.1016/S1361-8415(99)80030-9)
- Studholme C, Hill DLG, Hawkes DJ. An overlap invariant entropy measure of 3D medical image alignment. *Pattern Recognit* 1999; **32**: 71–86. doi: [https://doi.org/10.1016/S0031-3203\(98\)00091-0](https://doi.org/10.1016/S0031-3203(98)00091-0)
- Wang Y-H, Li G, Ma R-H, Zhao Y-P, Zhang H, Meng J-H, et al. Diagnostic efficacy of CBCT, MRI, and CBCT-MRI fused

- images in distinguishing articular disc calcification from loose body of temporomandibular joint. *Clin Oral Investig* 2021; **25**: 1907–14. doi: <https://doi.org/10.1007/s00784-020-03497-w>
26. Al-Saleh MAQ, Alsufyani NA, Lagravere M, Nebbe B, Lai H, Jaremko JL, et al. Mri alone versus MRI-CBCT registered images to evaluate temporomandibular joint internal derangement. *Oral Surg Oral Med Oral Pathol Oral Radiol* 2016; **122**: 638–45. doi: <https://doi.org/10.1016/j.oooo.2016.07.024>
27. Schnabl D, Rottler A-K, Schupp W, Boisserée W, Grunert I. Cbct and MRT imaging in patients clinically diagnosed with temporomandibular joint arthralgia. *Heliyon* 2018; **4**:e00641. doi: <https://doi.org/10.1016/j.heliyon.2018.e00641>
28. Widmalm SE, Brooks SL, Sano T, Upton LG, McKay DC. Limitation of the diagnostic value of Mr images for diagnosing temporomandibular joint disorders. *Dentomaxillofac Radiol* 2006; **35**: 334–8. doi: <https://doi.org/10.1259/dmfr/23427399>
29. Boveiri HR, Khayami R, Javidan R, Mehdizadeh A. Medical image registration using deep neural networks: a comprehensive review. *Computers & Electrical Engineering* 2020; **87**: 106767. doi: <https://doi.org/10.1016/j.compeleceng.2020.106767>